

# Capillary Surface Interfaces

Robert Finn

Anyone who has seen or felt a raindrop, or who has written with a pen, observed a spiderweb, dined by candlelight, or interacted in any of myriad other ways with the surrounding world, has encountered capillarity phenomena. Most such occurrences are so familiar as to escape special notice; others, such as the rise of liquid in a narrow tube, have dramatic impact and became scientific challenges. Recorded observations of liquid rise in thin tubes can be traced at least to medieval times; the phenomenon initially defied explanation and came to be described by the Latin word *capillus*, meaning hair.

It became clearly understood during recent centuries that many phenomena share a unifying feature of being something that happens whenever two materials are situated adjacent to each other and do not mix. We will use the term *capillary surface* to describe the free interface that occurs when one of the materials is a liquid and the other a liquid or gas. In physical configurations such as the capillary tube, interfaces occur also between these materials and rigid solids; these latter interfaces yield in many cases the dominant influence for determining the configuration.

In this article we describe a number of such phenomena, notably some that were discovered very recently as formal consequences of the highly nonlinear governing equations. These discoveries include discontinuous dependence on the boundary data, symmetry breaking, failure of existence

under physical conditions, and failure of uniqueness under conditions for which solutions exist. The predicted behavior is in some cases in striking variance with predictions that come from linearizations and formal expansions, sufficiently so that it led to initial doubts as to the physical validity of the theory. In part for that reason, experiments were devised to determine what actually occurs. Some of the experiments required microgravity conditions and were conducted on NASA Space Shuttle flights and in the Russian Mir Space Station. In what follows we outline the history of the problems and describe some of the current theory and relevant experimental results.

The original attempts to explain liquid rise in a capillary tube were based on the notion that the portion of the tube above the liquid was exerting a pull on the liquid surface. That, however, cannot be what is happening, as one sees simply by observing that the surface fails to recede (or to change in any way) if the tube is cut off just above the interface. Further, changing the thickness of the walls has no effect on the surface, thus suggesting that the forces giving rise to the phenomenon can be significant only at extremely small distances (more precise analysis indicates a large portion of these forces to be at most molecular in range). Thus, for a vertical tube the net attractive forces between liquid and wall must by symmetry be horizontal. It is this horizontal attraction that causes the vertical rise. Molecules being pulled toward the walls force other molecules aside in all directions, resulting in a spread along the walls that is only partly compensated by gravity. Liquid is forced upward along the walls, and cohesive forces

---

*Robert Finn is professor emeritus of mathematics at Stanford University. His e-mail address is [finn@gauss.stanford.edu](mailto:finn@gauss.stanford.edu).*

carry the remaining liquid column with it. The lowered hydrostatic pressure at the top of the column is compensated by the curvature of the surface, in essentially the same manner as occurs with a soap bubble. This basic observation as to the nature of the acting forces appears for the first time in the writings of John Leslie in 1802.

An early attempt to explain capillarity phenomena was made by Aristotle, who wrote circa 350 B.C. that *A broad flat body, even of heavy material, will float on a water surface, but a long thin one such as a needle will always sink.* Any reader with access to a needle and a glass of water will have little difficulty refuting the statement. On the other hand, Leonardo da Vinci wrote in 1490 on the mechanics of formation of liquid drops, using ideas very similar to current thinking. But in the absence of the calculus, the theory could not be made quantitative, and there was no convincing way to test it against experiments.

The achievements of the modern theory depend essentially on mathematical methods, and specifically on the calculus, on the calculus of variations, and on differential geometry. When one looks back on how that came about, one is struck by the irony that the initial mathematical insights were introduced by Thomas Young, a medical physician and natural philosopher who made no secret of his contempt for mathematics (and more specifically for particular mathematicians). But it was Young who in 1805 first introduced the mathematical concept of *mean curvature*  $H$  of a surface and who showed its importance for capillarity by relating it to the pressure change across the surface:  $\Delta p = 2\sigma H$ , with  $\sigma$  equal to surface tension. Young also reasoned that if the liquid rests on a support surface  $\mathcal{W}$ , then the fluid surface  $S$  meets  $\mathcal{W}$  in an angle  $\gamma$  (*contact angle*) that depends only on the materials and not on the gravity field, the shape of the surface, or the shape or thickness of  $\mathcal{W}$ ; see Figure 1.

Young derived with these concepts and from the laws of hydrostatics the first correct approximation for the rise height at the center of a circular capillary tube of small radius  $a$  immersed vertically in a large liquid bath:

$$(1) \quad u_0 \approx \frac{2 \cos \gamma}{\kappa a}, \quad \kappa = \frac{\rho g}{\sigma};$$

here  $\rho$  is the density change across the free surface,  $g$  the magnitude of gravitational acceleration. See Figure 2.

Young's chief competitor in these developments was Laplace, who relied heavily on mathematics. Laplace derived a formal mathematical expression

$$(2) \quad 2H \equiv \operatorname{div} Tu, \quad Tu \equiv \frac{Du}{\sqrt{1 + |Du|^2}}$$

for the mean curvature  $H$  of a surface  $u(x, y)$ ; he was led to

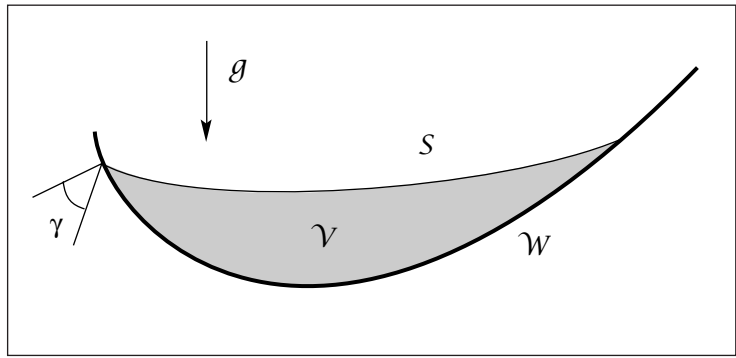


Figure 1. Fluid interface  $S$ , support surface  $\mathcal{W}$ ;  $\gamma$  is the angle between the two surface normals.

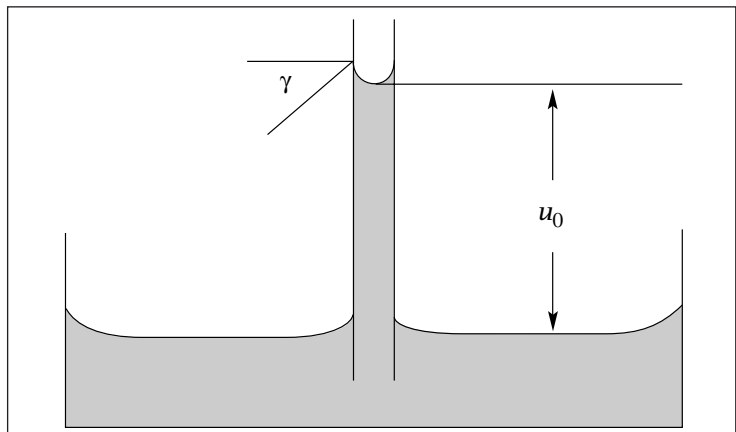


Figure 2. Capillary tube configuration.

**Theorem 1.** The height  $u(x, y)$  of a capillary surface interface lying over a domain  $\Omega$  in a vertical gravity field satisfies the differential equation

$$(3) \quad \operatorname{div} Tu = \kappa u + \lambda.$$

Here  $\lambda$  is a constant to be determined by physical conditions (such as fluid volume) and boundary conditions;  $\kappa$  is positive when the denser fluid lies below the interface; in the contrary case, the sign of  $\kappa$  reverses. For the problem described above, considered by Young,  $\lambda = 0$  and (3) becomes

$$(4) \quad \operatorname{div} Tu = \kappa u.$$

For a capillary surface in a cylindrical vertical tube of homogeneous material and general horizontal section  $\Omega$ , the Young condition on the contact angle yields the boundary condition

$$(5) \quad \nu \cdot Tu = \cos \gamma$$

on  $\Sigma = \partial\Omega$ , with  $\nu$  the unit exterior normal on  $\Sigma$ .

Instead of a tube dipped into an infinite reservoir as considered by Young, one could imagine a vertical tube closed at the bottom and partially filled with a prescribed volume of liquid covering the base. In general in this case  $\lambda \neq 0$ , but addition of a constant to  $u$  converts (3) to (4). From uniqueness properties discussed below, it follows that in

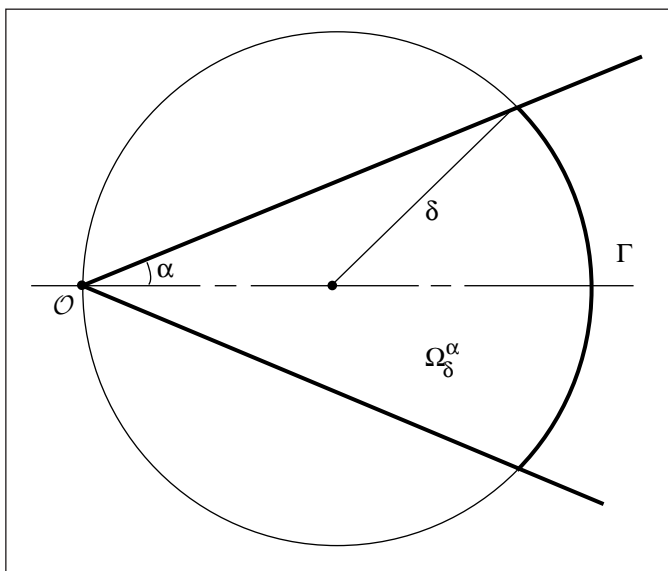


Figure 3. Wedge domain.

all cases, and independent of the volume of liquid, the surfaces obtained are geometrically the same. This result holds also when  $\kappa = 0$  and a solution exists; however, existence cannot in general then be expected, as we shall observe below. To some extent, these considerations extend to configurations with  $\kappa < 0$ , i.e., with the heavier fluid on top; however, in general both existence and uniqueness may fail when  $\kappa < 0$ .

If  $\gamma$  is constant, we may normalize it to the range  $0 \leq \gamma \leq \pi$ . The range  $0 \leq \gamma < \pi/2$  then indicates capillary rise;  $\pi/2 < \gamma \leq \pi$  yields capillary fall. It suffices to consider the former case, as the other can be reduced to it. If  $\gamma = \pi/2$ , the only solutions of (4), (5) with  $\kappa > 0$  are the surfaces  $u \equiv 0$ ; if  $\kappa = 0$ , the only such surfaces are  $u \equiv \text{const.}$  If  $\kappa < 0$ , nontrivial such solutions appear.

With the aid of (4) and (5), Laplace could improve the approximation (1) to

$$(6) \quad u_0 \approx \frac{2 \cos \gamma}{\kappa a} - \left( \frac{1}{\cos \gamma} - \frac{2}{3} \left( \frac{1 - \sin^3 \gamma}{\cos^3 \gamma} \right) \right) a.$$

Laplace did not prove this formula completely, nor did he provide any error estimates, and in fact it was disputed in later literature. Note that the right side of (6) becomes negative if the nondimensional “Bond number”  $B = \kappa a^2 > 8$ , in which case the estimate gives less information than does (1). The formula is, however, asymptotically correct for small  $B$ ; that was proved for the first time almost two centuries later in 1980 by David Siegel, who also provided explicit error bounds; a proof yielding improved bounds was given by the present author in 1984, and further improvements were obtained by Siegel in 1989. The expression (6) was extended by P. Concus (1968) to the entire traverse  $0 < r < a$ . F. Brulois in 1981 provided the full asymptotic expansion in powers of  $B$ ; that re-

sult was obtained again independently by E. Miersemann in 1994.

In 1830 Gauss used the *Principle of Virtual Work*, formulated by Johann Bernoulli in 1717, to unify the achievements of Young and of Laplace, and he obtained both the differential equation and the boundary condition as consequences of the principle. In the Gauss formulation the constant  $\lambda$  in (3) appears as a Lagrange parameter arising from an eventual volume constraint.

Capillarity attracted the attention of many of the leading mathematicians of the nineteenth and early twentieth centuries, and some striking results were obtained; however, the topic then suffered a hiatus till the latter part of the present century. A great influence toward new discoveries was provided by the “BV theory”, developed originally for minimal surfaces by E. de Giorgi and his co-workers. In the context of this theory M. Emmer provided in 1973 the first existence theorem for the capillary tube of general section. For further references to these developments, see [1, 2]. Other directions were initiated by Almgren, Federer, Fleming, Simons, and others and led to results of different character; see, e.g., [10].

### The Wedge Phenomenon

It is unlikely that anyone reading this article will be unfamiliar with the name of Brook Taylor, as the Taylor series figures prominently in every calculus sequence. It is less widely known that Taylor made capillarity experiments, almost one hundred years prior to the work of Young and of Laplace. He formed a vertical wedge of small angle  $2\alpha$  between two glass plates and observed that a drop of water placed into the corner would rise up into the wedge, forming contact lines on the plates that tend upward in a manner “very near to the common hyperbola”. Taylor had no theory to explain the phenomenon, but in the course of the ensuing centuries a number of “proofs” of results leading to or at least suggesting a hyperbolic rise independent of opening angle appeared in the literature.

The actual behavior is quite different and varies dramatically depending on the contact angle and angle of opening. *There is a discontinuous transition in behavior at the crossing point  $\alpha + \gamma = \pi/2$ .* In the range  $\alpha + \gamma < \pi/2$ , Taylor’s observation is verified as a formal property that holds for any solution. Specifically, we consider a surface  $S$  given by  $u(x, y)$  over the intersection  $\Omega_\delta^\alpha$  of a wedge domain with a disk of radius  $\delta$  as in Figure 3. We obtain:

**Theorem 2.** *Let  $u(x, y)$  satisfy (4) with  $\kappa > 0$  in  $\Omega_\delta^\alpha$  and suppose  $S$  meets interior points of the bounding wedge walls in an angle  $\gamma$  such that  $\alpha + \gamma < \pi/2$ . Let  $k = \sin \alpha / \cos \gamma$ . Then in terms of a polar coordinate system  $(r, \theta)$  centered at the vertex  $O$ , there holds*

$$(7) \quad u \approx \frac{\cos \theta - \sqrt{k^2 - \sin^2 \theta}}{k\kappa r}.$$

On the other hand, if  $\alpha + \gamma \geq \pi/2$ , then  $u(x, y)$  is bounded, depending only on  $\kappa$  and on the size of the domain covered by  $S$  near  $\mathcal{O}$ :

**Theorem 3.** *If  $u(x, y)$  satisfies (4) with  $\kappa > 0$  in  $\Omega_\delta^\alpha$  and if  $S$  meets the bounding wedge walls in an angle  $\gamma$  such that  $\alpha + \gamma \geq \pi/2$ , then*

$$(8) \quad |u| \leq (2/\kappa\delta) + \delta$$

throughout  $\Omega_\delta^\alpha$ .

It is important to observe that the boundary is singular at  $\mathcal{O}$  and the contact angle cannot be prescribed there. Despite this singularity, neither theorem requires any growth hypothesis on the solution near  $\mathcal{O}$ . Such a statement would not be possible, for example, for harmonic functions under classical conditions of prescribed values or normal derivatives on the boundary. It is also noteworthy that no hypothesis is introduced with regard to behavior on  $\Gamma$ . The local behavior is completely controlled by the opening angle and by the contact angle over the wedge segments near  $\mathcal{O}$  and is an essential consequence of the nonlinearity in the equation. (In another direction, it can be shown that if  $u(x, y)$  satisfies (4) in all space, then  $u \equiv 0$ .)

If in an initial configuration there holds  $\alpha + \gamma > \pi/2$  and  $\alpha$  is then continuously decreased until equality is attained, (8) provides a uniform bound on height up to and including the crossing point. For any smaller  $\alpha$  the estimate (7) prevails, and the surface is unbounded at  $\mathcal{O}$ .

This behavior was tested in the Stanford University medical school in a “kitchen sink” experiment by T. Coburn, using two acrylic plastic plates and distilled water. Figure 4 shows the result of a change of about  $2^\circ$  in the angle between the plates, leading in the smaller  $\alpha$  case to a measured rise height over ten times the predicted maximum of Theorem 2. That result was confirmed under controlled laboratory conditions and for varying materials by M. Weislogel in 1992; it yields a contact angle of water with acrylic plastic of  $80^\circ, \pm 2^\circ$ . (See the remarks in the next section.)

The relation (7) was extended by Miersemann (1993) to a complete asymptotic expansion at  $\mathcal{O}$ , in powers of  $B = \kappa r^2$ . It is remarkable that *the coefficients are completely characterized by  $\alpha$  and  $\gamma$  and are otherwise independent of the data and domain of definition for the solution*. Thus again the behavior is strikingly different from that arising in linear problems.

If gravity vanishes, the discontinuous dependence becomes still more striking. In this case (3) becomes

$$(9) \quad \operatorname{div} Tu = \lambda = 2H,$$

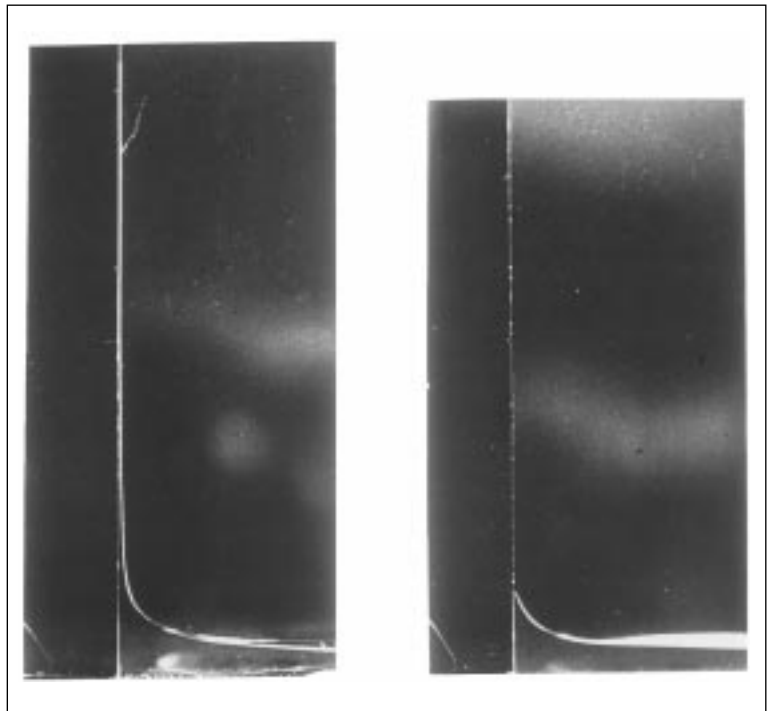


**Figure 4.** Water rise in wedge of acrylic plastic. (Left)  $\alpha + \gamma < \pi/2$ . (Right)  $\alpha + \gamma \geq \pi/2$ .

so that the surface has constant mean curvature. We find:

**Theorem 4.** *If  $u(x, y)$  satisfies (9) in  $\Omega_\delta^\alpha$  and defines a surface  $S$  that meets interior points of the wedge walls in the constant angle  $\gamma$ , then  $\alpha + \gamma \geq \pi/2$  and  $u(x, y)$  is bounded at  $\mathcal{O}$ .*

Thus, the change is now from boundedness to nonexistence of a solution.

It may at first seem strange that this physical problem should fail to admit a solution; after all, fluid placed into a container has to go someplace. Figure 5 shows the result of an experiment conducted by W. Masica in the 132-meter drop tower facility at NASA Glenn Research Center, which provides about five seconds of free fall. Two cylindrical containers of regular hexagonal section were dropped, both with acrylic plastic walls but with differing liquids, providing configurations on both sides of the critical value. In this case, when  $\alpha + \gamma \geq \pi/2$ , the exact solution is known as a lower spherical cap, and this surface is observed in the experiment. When  $\alpha + \gamma < \pi/2$ , the liquid fills out the edges and climbs to the top of the container, as indicated in Figure 6. Thus the physically observed surface folds back over itself and cannot be expressed as a graph over the prescribed domain. The physical surface thus exists as it has to, but not in the form of a solution to (9), (5). It should be noted that *for regular polygonal sections, the change in character of the solution is discontinuous*. That is clearly apparent, as (unique) solutions exist as lower spherical caps throughout the closed range  $\alpha + \gamma \geq \pi/2$ .

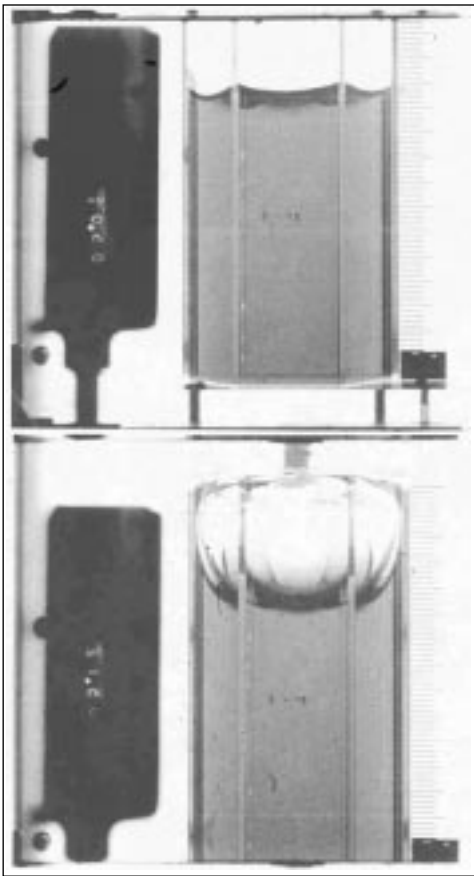


**Figure 5. Liquids with different contact angle in acrylic plastic cylinders of hexagonal section during free fall. (Top)  $\alpha + \gamma > \pi/2$ . (Bottom)  $\alpha + \gamma < \pi/2$ .**

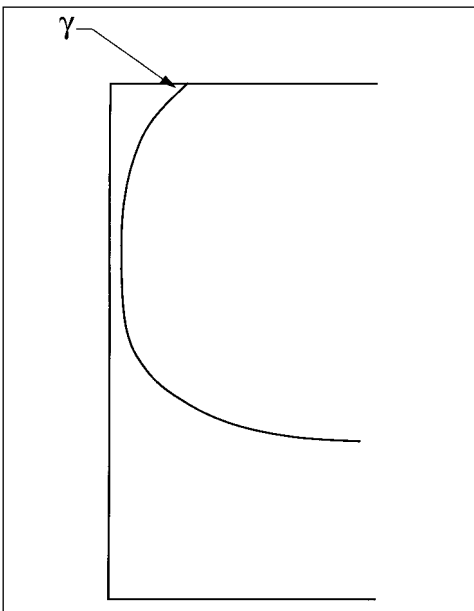


**Figure 6. Sketch of side view at edge in drop tower experiment,  $\alpha + \gamma < \pi/2$ .**

### Existence and Nonexistence; the Canonical Proboscis

The just-described concurrence of experimental results with prediction from the formal theory provides a persuasive indication that the Young-Laplace-Gauss theory, beyond its aesthetic appeal, also correctly describes physical reality. The physical validity of that theory has been questioned on the basis of ambiguities that occur in attempts to measure contact angle. There are experimental procedures that give rise to reasonably repeatable measurements of what may be described as an “equilibrium angle”. However, if one partially fills a vertical circular cylinder with liquid (symmetrically) and then tries to move the liquid upward by a piston at the bottom, the contact line of liquid with solid does not immediately move, but instead an increase in the contact angle is observed. The maximum possible such angle before motion sets in is known as the “advancing angle”. Correspondingly, the smallest such angle obtainable before reverse motion occurs is the “receding angle”. The difference between advancing and receding angles is the “hysteresis range”, which presumably arises due to frictional resistance to motion at the interface, but could conceivably also reflect inadequacy of the theory. This range can be very large;

for example, for the water and acrylic plastic interface in the Coburn experiment described above, it is over  $20^\circ$ . Such apparent anomalies of measurement have led to some questioning of “contact angle” as a physical concept. The experimental confirmation of discontinuous dependence on data at the critical opening in a wedge supports the view that contact angle does have intrinsic physical meaning; in addition it suggests a new method for measuring the angle in particular cases. One need only place a drop of the liquid into a wedge that is formed by vertical plates of the solid and has initial opening sufficiently large that Theorem 3 applies. The opening angle is then slowly decreased until the liquid jumps up in the corner to a height above the bound given by (8). The criteria of Theorems 2 and 3 then determine  $\gamma$ .

For values of  $\gamma$  close to  $\pi/2$ , remarkably good agreement has been obtained in this way with the “equilibrium angle” measured under terrestrial conditions. On the other hand, for values of  $\gamma$  close to  $0^\circ$ , the physical changes occur in the immediate neighborhood of  $\mathcal{O}$  with an opening close to  $\pi$ , and measurements become subject to experimental error. We thus seek domains in which the discontinuous behavior is manifested over a larger set. We can do so in the context of a general theory of independent mathematical interest, applying to zero gravity configurations and determining criteria for existence and nonexistence of solutions of (9), (5) in tubes of general piecewise smooth section  $\Omega$ .

Let  $\Gamma$  be a curve in  $\Omega$  cutting off a subdomain  $\Omega^* \subset \Omega$  and subarc  $\Sigma^* \subset \Sigma = \partial\Omega$ , as in Figure 7. From the zero gravity equations (9) and (5) we obtain, for the area  $|\Omega^*|$  and length  $|\Sigma^*|$ ,

$$(10) \quad 2H|\Omega^*| = |\Sigma^*| \cos \gamma + \int_{\Gamma} \mathbf{v} \cdot T \mathbf{u} \, ds.$$

The same procedure with  $\Omega^* = \Omega$  yields

$$(11) \quad 2H = \frac{|\Sigma| \cos \gamma}{|\Omega|}.$$

In (10) we observe that

$$(12) \quad |\mathbf{v} \cdot T \mathbf{u}| \leq \frac{|Du|}{\sqrt{1 + |Du|^2}} < 1$$

for any differentiable function  $u(x, y)$ . It follows that whenever there exists a solution to the problem, the functional  $\Phi(\Omega^*; \gamma) \equiv |\Gamma| - |\Sigma^*| \cos \gamma + 2H|\Omega^*|$  satisfies

$$(13) \quad \Phi(\Omega^*; \gamma) > 0$$

for all strict nonnull subsets  $\Omega^* \subset \Omega$  cut off by smooth curves  $\Gamma$ , when  $H$  is determined by (11). This inequality provides a necessary condition for existence of a solution.

To make the condition sufficient, we appeal to the properties of “Caccioppoli sets” in the BV

theory. Roughly speaking, these are subsets of  $\Omega$  whose boundaries within  $\Omega$  can be assigned a finite length, in a variational sense. Details of general properties of these sets can be found in [1, 2]; reference [3] and references cited there give specific applications to capillarity. It was shown by Giusti in 1976 that if we rephrase (13) as a property of Caccioppoli sets, the condition also becomes sufficient; see also Theorem 7.10 of [3]. We obtain:

**Theorem 5.** *A smooth solution  $u(x, y)$  exists in  $\Omega$  if and only if the functional  $\Phi(\Omega^*; \gamma)$  is positive for every Caccioppoli set  $\Omega^* \subset \Omega$ , with  $\Omega^*$  not equal to  $\emptyset$  or  $\Omega$ .*

In order to use this result, one proves that if  $\Omega$  is piecewise smooth, then  $\Phi$  can be minimized among Caccioppoli sets, and the minimizing sets can be characterized geometrically. One obtains:

**Theorem 6.** *For  $\Omega$  piecewise smooth, there exists at least one minimizing set  $\Omega_0$  for  $\Phi$  in  $\Omega$ . Any such set is bounded within  $\Omega$  by a finite number  $N_0$  of nonintersecting subarcs of semicircles of radius  $1/(2H)$ , each of which either meets  $\Sigma$  at a smooth point with angle  $\gamma$  measured within  $\Omega_0$  or meets  $\Sigma$  at a corner point. The curvature vector of each subarc is directed exterior to  $\Omega_0$ .*

Thus, the existence question is reduced to evaluation of particular configurations, which often can be determined explicitly by the geometrical requirements of prescribed radius and angle with  $\Sigma$ . In general, there will be a number  $N \geq N_0$  of subarcs of semicircles satisfying those requirements. We refer to these arcs as *extremals*. If  $N = 0$ , then since  $\Phi$  vanishes on the null set, we find  $\Phi(\Omega^*; \gamma) > 0$ , all  $\Omega^* \subset \Omega$  with  $\Omega^* \neq \emptyset, \Omega$ , and hence by Theorem 5 a smooth solution exists. That happens, for example, in a rectangle when  $\gamma \geq \pi/4$ . (If  $\gamma < \pi/4$ , then by Theorem 4 there is no solution for that problem.)

If  $N$  is finite and positive, then a finite number of subdomains  $\Omega^*$  appears for examination. If one or more of these sets yields  $\Phi \leq 0$ , then no solution of (9), (5) can exist in  $\Omega$ . If the value zero but no smaller value is achieved by  $\Phi$  on the sets  $\Omega^*$ , then there exists a set  $\Omega_0$  among them such that there will be a solution  $u(x, y)$  in the set  $\Omega \setminus \Omega_0$  and such that  $u \rightarrow \infty$  as  $\Omega_0$  is approached from within  $\Omega \setminus \Omega_0$ . If we then set  $u \equiv \infty$  in  $\Omega_0$ , we obtain a generalized solution in a sense introduced by M. Miranda in connection with minimal surfaces in 1977. This solution will have mean curvature determined by (11).

If a domain  $\Omega^*$  exists with  $\Phi(\Omega^*; \gamma) < 0$ , then that inequality holds also for each minimizer. Again it can be shown [4] that there exists a solution  $u(x, y)$  in a subdomain such that  $u(x, y)$  tends to infinity on a finite number of circular subarcs of equal radius that intersect  $\Sigma$  in angle  $\gamma$ . The

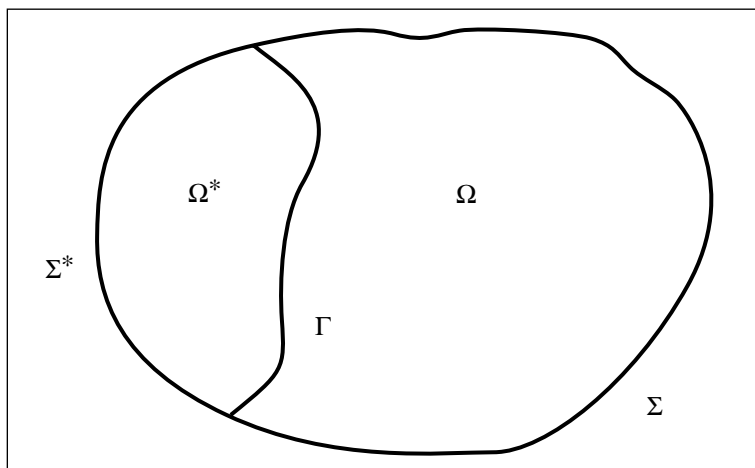


**Figure 7.** Existence criterion;  $\Omega^*$  is the portion of  $\Omega$  cut off by an arbitrary curve  $\Gamma$ .

mean curvature  $H$  (and accordingly the radius of the arcs) will, however, no longer be determined by (11).

The case  $N = N_0 = \infty$  can occur, and it is this case that provides the clue for obtaining domains in which there is abrupt transition in height of solutions over large sets at the critical angle separating existence from nonexistence. Following joint work by Bruce Fischer, by Tanya Leise, and by Jonathan Marek with the author, we look for a translational continuum of extremals, each of which yields  $\Phi = 0$ . We construct the domain  $\Omega$  by finding the curves that meet a given translational family of circular arcs of common radius  $R$  in a fixed angle  $\gamma_0$ ; these curves can be written explicitly, in the form

$$(14) \quad x + c = \sqrt{R^2 - y^2} + R \sin \gamma_0 \ln \frac{\sqrt{R^2 - y^2} \cos \gamma_0 - y \sin \gamma_0}{R + y \cos \gamma_0 + \sqrt{R^2 - y^2} \sin \gamma_0}.$$

We choose upper and lower branches of the curves joining at a point on the  $x$ -axis as part of the boundary  $\Sigma$ , and then complete the domain by a circular "bubble" whose radius is adjusted so that the arcs become extremals with  $\Phi = 0$ , as indicated in Figure 8. We refer to such a domain as a *canonical proboscis*. It can be shown that when the contact angle exceeds  $\gamma_0$ , then a smooth solution of (9), (5) exists for that domain; however, for  $\gamma = \gamma_0$  the surface becomes a generalized solution in the sense of Miranda, infinite in the entire region covered by the extremals.

Since the relative size of the portion of such a domain that is covered by extremals can be made as large as desired, the canonical proboscides can be used for determining small contact angles based on rapid changes of fluid height over large sets (see the initial paragraph of this section). The theory was tested by Fred W. Leslie in the Space Shuttle USML-2 using containers with two proboscides on

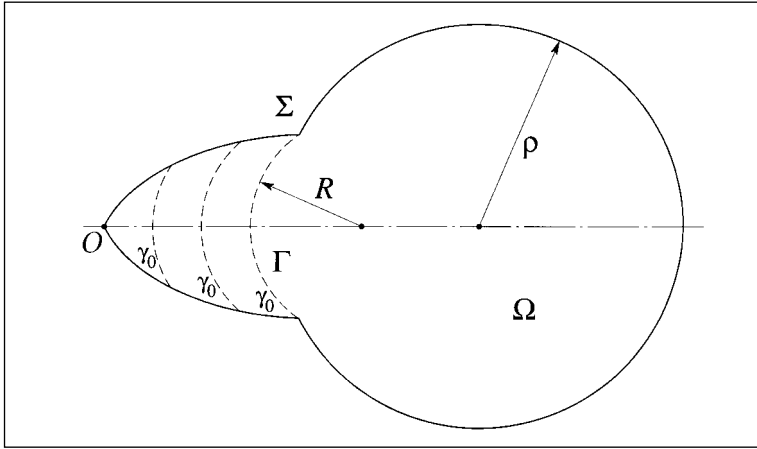


Figure 8. Proboscis domain with bubble showing extremals  $\Gamma$ .

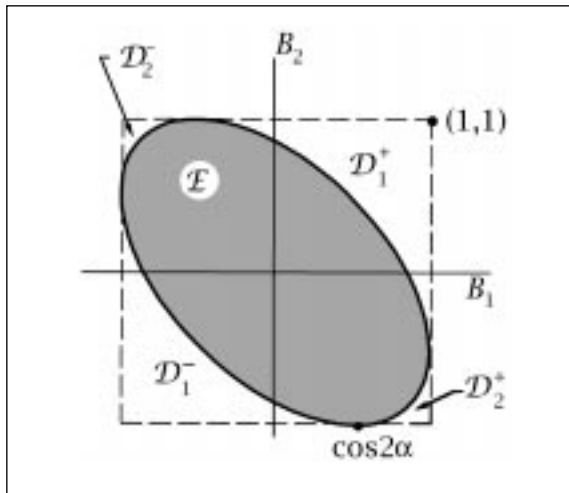


Figure 10. Ellipse of regularity.

opposite sides of a “bubble” corresponding to contact angles  $30^\circ$  and  $34^\circ$ . The fluid used had an equilibrium contact angle measured on Earth as  $32^\circ$ , with a hysteresis range of  $25^\circ$ . Effects of resistance of the contact line to motion (see beginning of this section) were observed in the experiment, but after the astronaut tapped the apparatus the successive configurations of Figure 9 (top row in cover montage) appeared. In an analogous container stored for some days, the fluid on the right climbed over the top and descended on the other side. Thus, although time is required (and perhaps also thermal and mechanical fluctuations), the resistance effects are overcome and a clearly determined contact angle is evidenced.

### Differing Contact Angles; the $\mathcal{D}_2^\pm$ Domains, and Edge Blobs

We return to the discussion of wedges above and ask what happens when two distinct contact angles  $\gamma_1, \gamma_2$  are prescribed on the two sides of a wedge. Again, new differences in possible behavior appear. Setting  $B_j = \cos \gamma_j$ , one sees easily that a necessary condition for existence of any surface over a wedge domain  $\Omega^\alpha$  of opening  $2\alpha$  and with

normal vector continuous to  $\mathcal{O}$  is that  $(B_1, B_2)$  lies in the closed ellipse

$$(15) \quad \mathcal{E} : B_1^2 + B_2^2 + 2B_1B_2 \cos 2\alpha \leq \sin^2 2\alpha.$$

See Figure 10. For data in the indicated domains  $\mathcal{D}_1^\pm$  bounded between the square and the ellipse, one can show the natural extension of Theorem 4 that solutions of (9), (5) are precluded without regard to growth hypotheses.

For data lying in  $\mathcal{D}_2^\pm$  the situation is very different. In this case solutions of (9), (5) have been shown to exist under general conditions, but their form must be very different from what occurs for data in  $\mathcal{E}$ , in which case spherical surfaces yield particular solutions; that cannot happen in  $\mathcal{D}_2^\pm$ , as the normal is discontinuous for such data. The classical Scherk minimal surface provides a particular example. But for data  $(B_1, B_2)$  that are not on the boundary of the square in Figure 10, the solution  $u(x, y)$  is bounded above and below. It has been conjectured by J-T. Chen, E. Miersemann, and this author that  $u(x, y)$  is itself discontinuous at  $\mathcal{O}$ . The conjecture was examined numerically, initially in special cases by Concus and Finn (1994), and later by Mittelman and Zhu (1996) in a comprehensive survey of minimal surfaces achieving the data  $(B, -B)$  and  $(-B, B)$  on adjacent sides of a square. The calculations suggest that a discontinuity does indeed appear in  $\mathcal{D}_2^\pm$ , although at points close to the boundary with  $\mathcal{E}$  it was so small as to create a numerical challenge to find it.

The local problem we have been discussing can be realized either by a global surface in a capillary tube, with prescribed contact angle along the walls, or alternatively by a drop of liquid sitting in a wedge with planar walls that meet in a line  $\mathcal{L}$  and extend to infinity. In the latter case, if data come from  $\mathcal{E}$ , a solution can be given explicitly for any prescribed  $H > 0$ , as the outer spherical surface  $S$  of a portion of a ball of radius  $1/H$  cut off by the wedge. This is effectively the only possible such surface. Specifically:

**Theorem 7.** *If  $(B_1, B_2)$  lies interior to  $\mathcal{E}$  and if  $S$  is topologically a disk and locally a graph near its intersections with  $\mathcal{L}$ , over a plane  $\Pi$  orthogonal to  $\mathcal{L}$ , then  $S$  is metrically spherical, and is uniquely determined by its volume, up to rigid motion parallel to  $\mathcal{L}$ .*

Theorem 7 can be viewed as an extension of the H. Hopf theorem that characterizes genus zero immersions of closed constant  $H$  surfaces as metric spheres.

We now keep the volume of the drop constant and allow the data to approach the boundary of  $\mathcal{E}$ . For simplicity we restrict attention to the two symmetry lines  $B_1 = B_2$  joining the  $\mathcal{D}_1^\pm$  regions, and  $B_1 = -B_2$  joining the  $\mathcal{D}_2^\pm$  regions. We find:



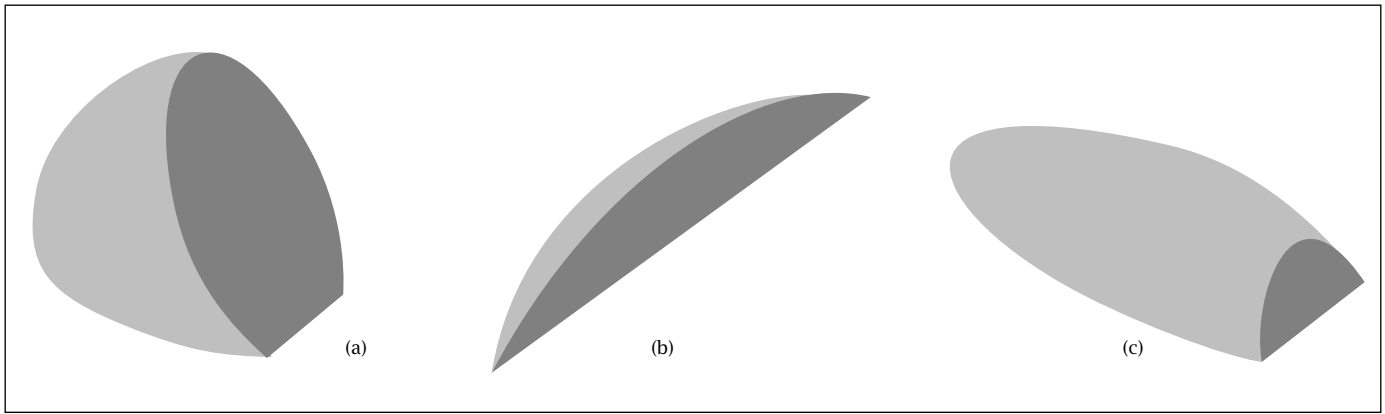


**Figure 11. Spherical blobs in a wedge of opening  $2\alpha = 50^\circ$  for three choices of data near boundary of  $\mathcal{E}$ .** (a) Data in  $\mathcal{E}$  near  $\mathcal{D}_1^-$ ; crossing the boundary into  $\mathcal{D}_1^-$  yields continuous transition to a sphere with two caps removed. (b) Data near  $\mathcal{D}_1^+$ ; transition to boundary yields spread extending to infinity along edge. Transition across boundary not possible. (c) Data near  $\mathcal{D}_2^\pm$ ; transition across boundary yields fictitious drop realized physically as drop on single plane.

**Theorem 8.** As one increases  $B_1 = B_2$  to move from the ellipse  $\mathcal{E}$  to the region in the parameter space  $\mathcal{D}_1^-$ , the free surface of the drop changes in topological character from a disk to a cylinder. The surface becomes a metric sphere with two caps removed at the places where the drop contacts the two plates. Figure 11a depicts a value of the parameter shortly before the transition occurs. On approaching  $\mathcal{D}_1^+$  within  $\mathcal{E}$  on the same line, the radius of the drop grows unboundedly, with the drop covering very thinly a long segment of  $\mathcal{L}$ ; see Figure 11b. As either  $\mathcal{D}_2^-$  or  $\mathcal{D}_2^+$  are entered from  $\mathcal{E}$  on the line  $B_1 = -B_2$ , the drop becomes a spherical cap lying on a single plate and not contacting the other plate; see Figure 11c.

As already mentioned, for data in  $\mathcal{D}_1^-$  or in  $\mathcal{D}_1^+$  no drop in the wedge can exist even locally as a graph over a plane orthogonal to  $\mathcal{L}$ . Theorem 8 suggests that the same result should hold for  $\mathcal{D}_2^\pm$  data. The statement is here, however, less clear-cut; in fact, recent joint work of P. Concus, J. McCuan, and the author [6] shows that capillary surfaces with data in  $\mathcal{D}_2^\pm$  can exist locally as graphs. The matter may be related to the presence of vertices, in a sense introduced in [5]. There a blob of liquid topologically a ball was considered, resting on a system of planes, each of which it meets in a prescribed angle. Points at which intersection lines of the planes meet the surface of the blob are called *vertices*. This concept extends also to configurations in which the intersection point is not clearly defined, as can occur for data in  $\mathcal{D}_2^\pm$ . The following results are proved, for a configuration with  $N$  vertices, and for which all data on intersecting planes that it contacts lie in  $\mathcal{E}$ :

**Theorem 9.** If  $N \leq 2$ , then either  $N = 0$  and the blob consists either of a spherical ball or a spherical cap resting on a plane, or else  $N = 2$  and the blob forms a spherical drop in a wedge. If  $N = 3$ , then the blob covers the corner point of a trihedral angle; under

the supplementary orientation condition that the mean curvature vector is directed away from the vertex, the surface is spherical.

If  $N > 3$ , the surface need not be spherical. The surfaces described in the Appendix of [6] have four vertices. A spherical drop in a wedge has two vertices. We are led to:

**Conjecture.** There exists no blob in a wedge, with  $N = 2$  vertices and data in  $\mathcal{D}_2^\pm$ .

### Stability of Liquid Bridges I

A substantial literature has developed in recent years on stability criteria for liquid bridges joining two parallel plates separated by a distance  $h$ , in the absence of gravity. Earlier papers considered bridges joining prescribed circular rings, but more recently the problem was studied with contact angle conditions on the two plates. The initial contributions to this latter problem, due to M. Athanassenas and to T. I. Vogel, were for contact angles  $\gamma_1 = \gamma_2 = \pi/2$  for which a bridge exists as a circular cylinder, and established that every stable configuration is a cylinder with volume  $\mathcal{V} \geq h^3/\pi$ . A consequence is that instability occurs at half the value of  $h$  that is indicated in classical work of Plateau and of Rayleigh on stability of liquid columns. The discrepancy arises because of the use here of a contact angle condition, rather than the Dirichlet condition employed by those authors. It was later shown by Vogel and this author that the same inequality holds regardless of contact angles. The most complete results on stability of such bridges are due to Lianmin Zhou in her 1996 Stanford University dissertation; Zhou established in the general case of equal contact angles  $\gamma$  on the plates that regardless of  $\gamma$  there is a unique stable bridge if the volume exceeds a critical  $\mathcal{V}_\gamma$ . In 1997 Zhou also obtained the striking result that for unequal contact angles, the stability set in terms of a defining parameter can be disconnected.



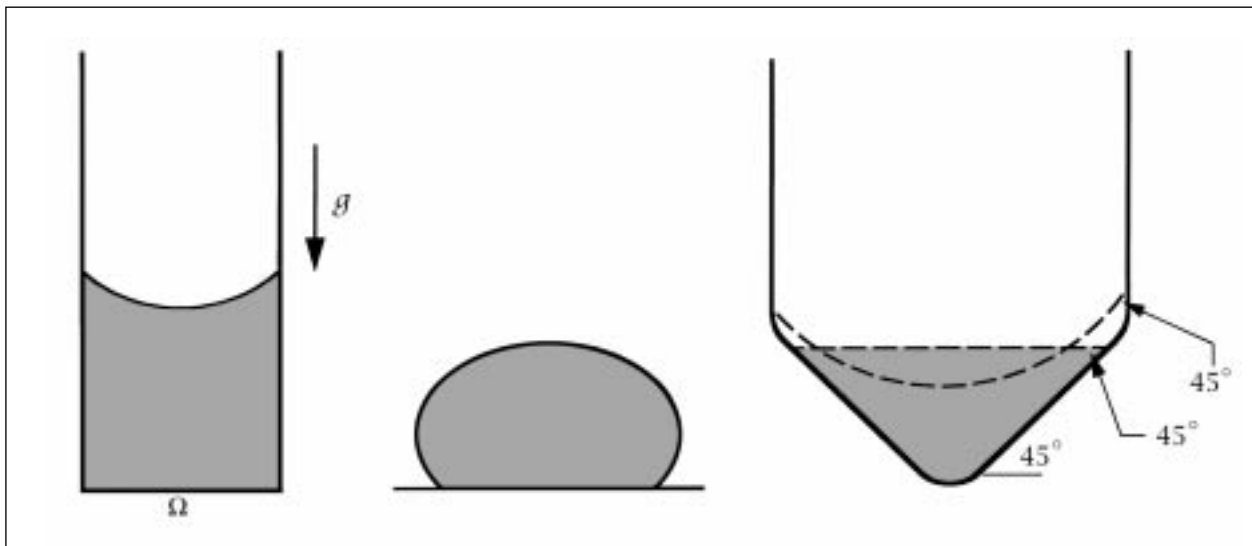


**Figure 12.** For given volume, uniqueness holds in cylindrical tube for any section  $\Omega$ ; also drop on plane is unique. But uniqueness fails in tube with curved bottom.

With regard to interpretation of these and also of earlier results, see the editor's note following her 1997 paper and the later clarifying papers by Große-Brauckmann and by Vogel. The stability criteria just described should also be interpreted in the context of the comments directly following:

### Stability of Liquid Bridges II

Stable liquid bridges joining parallel plates are rotationally symmetric but are in general not spherical. The meridional sections (profiles) of these surfaces were characterized by Delaunay in 1841 as the "roulades" of conic sections, and yield the sphere as a limiting case. We obtain, however, the result [6]: *Every nonspherical tubular bridge joining parallel plates is unstable, in the sense that it changes discontinuously with infinitesimal tilting of either plate.* In the earlier stability results, tilting of the plates was not contemplated.

From another point of view, there is the remarkable 1997 result of McCuan:

**Theorem 10.** *If the data  $(B_1, B_2)$  are not in  $\mathcal{D}_1^-$ , then there is no embedded tubular bridge joining intersecting plates.*

It should be noted here that data in  $\mathcal{D}_1^-$  are exactly those for which tubular bridges that are metrically spheres are possible (cf. Theorem 8 above). It is not known whether nonspherical embedded bridges can occur in that case. H. C. Wentz gave an example of a nonspherical immersed bridge, with contact angle  $\pi/2$  on both plates (and thus with data in  $\mathcal{E}$ ).

### Exotic Containers; Symmetry Breaking

For solutions of (3), (5) in a bounded domain  $\Omega$  with given  $\kappa \geq 0$ , uniqueness for prescribed fluid volume and contact angle can be established under much weaker conditions than are needed for linear equations. In fact, *arbitrary changes of the*

*data on any set of linear Hausdorff measure zero on  $\partial\Omega$  have no effect on the solution within  $\Omega$ ; this behavior holds without growth condition on the solutions considered.* Finn and Hwang showed if  $\kappa > 0$  (positive gravity) then *the stated result can be extended to unbounded domains of any form, without conditions at infinity.* In the case of equations (9), (5) (zero gravity), uniqueness can fail for unbounded domains.

A liquid blob resting on a planar support surface is also uniquely determined by its volume and contact angle, although the known proof proceeds along very different lines from the one for the statement above. We may ask whether uniqueness will persist during a continuous (convex) deformation of the plane to a tube. The negative answer can be seen from Figure 12. If the tube on the right is filled from the bottom until nearly the maximum height of the conical portion with a liquid making contact angle  $45^\circ$ , then a horizontal surface will result. But if it is filled to a very large height, then a curved meniscus appears. Removal of liquid can then lead to two distinct surfaces with identical volumes and contact angles.

This line of thought can be carried further:

Capillary surfaces are characterized as stationary configurations for the functional consisting of the sum of their mechanical (gravitational and surface) energies. In any gravity field and for any  $\gamma$ , *"exotic" containers can be constructed that yield an entire continuum of stationary interfaces for fluid configurations with the container as support surface, all with the same volume and the same mechanical energy.* This can be done in a rotationally symmetric container, so that all the surface interfaces have the same rotational symmetry, that no other symmetric capillary interfaces exist, and in addition so that energy can be decreased by a smooth asymmetric deformation of one of the surfaces. Thus, none of the interfaces in the

continuum can minimize the energy. Using a theorem due to Jean Taylor, we can prove that: *A minimizer for energy will exist but is necessarily asymmetric.*

Local minimizers for this “symmetry breaking” phenomenon were obtained computationally by Callahan, Concus, and Finn, and then sought experimentally, initially in drop tower experiments conducted by M. Weislogel. In the lower left of the cover montage are shown calculated meridian sections for the continuum of stationary symmetric nonminimizing surfaces, corresponding to a contact angle of  $80^\circ$  and zero gravity. The second row of the montage shows the planar initial interface in the earth’s gravity field, and a “spoon” shaped configuration that appeared near the end of free fall in the 132-meter drop tower. The spoon surface has the general form of the global minimizer suggested by the calculations, which had also located two local minimizers of larger energy (“potato chip” and “lichen”). The time permitted by the drop tower was, however, insufficient to determine whether the spoon configuration was in equilibrium or whether it might continue to evolve to some distinct further form.

In view of the ambiguity in the drop tower results, space experiments were later undertaken in order to obtain a more extended low gravity environment. These were performed initially by Lawrence de Lucas on the NASA Space Shuttle USML-1 and then by Shannon Lucid in the Mir Space Station. Figure 13 (the lower right corner of the cover montage) shows comparison of calculation with the latter experiment. The upper row shows the calculated spoon and potato chip; the lower row shows experimental observation. The experiment thus confirms both the occurrence and the qualitative structure of global and also of local asymmetric minimizers, in a container for which an entire continuum of symmetric stationary surfaces appears.

### Re-entrant Corners; Radial Limits

It was shown by Korevaar in 1980 that if the opening  $2\alpha$  of a wedge domain exceeds  $\pi$ , then even if  $B_1 = B_2$ , solutions  $u(x, y)$  of (3) can exist that are discontinuous at the vertex  $\mathcal{O}$ , in the sense that the tangential limits along the two sides can differ. Lancaster and Siegel (1996) showed that under general conditions radial limits at the vertex exist from every direction. Further, if  $u(x, y)$  is discontinuous, then there will exist “fans” of constant radial limit adjacent to each side. If  $2\alpha < \pi$  and if  $(B_1, B_2) \in \mathcal{E}$ , then the fans overlap, yielding continuity of  $u(x, y)$  up to  $\mathcal{O}$ . Earlier work, initially for the case  $B_1 = B_2$ , due originally to L. Simon and later extended by Tam, by Lieberman, and by Miersemann, can be used to extend the result to the parts of  $\partial\mathcal{E}$  bordering  $D_1^\pm$ , yielding continuity of the unit normal up to  $\mathcal{O}$ , and shows that for data in-

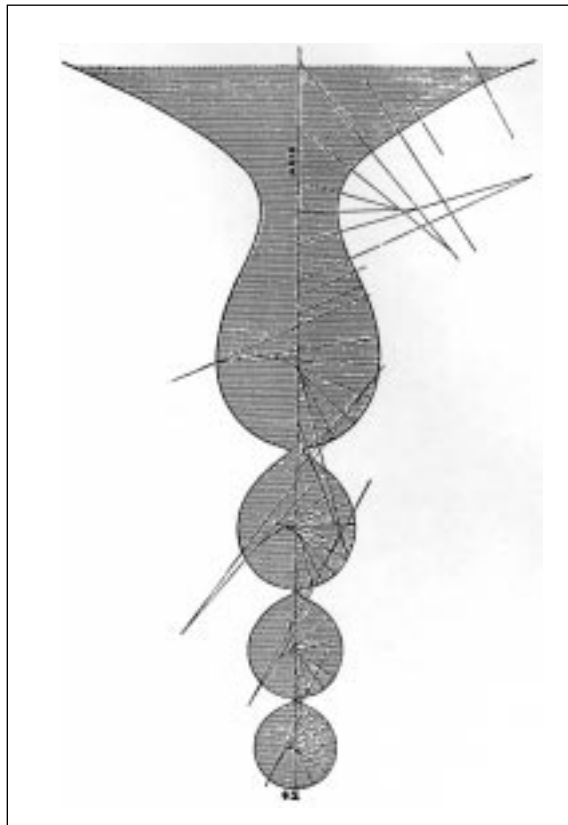


**Figure 14. Pendent liquid drop (Thomson, 1886).**

terior to  $\mathcal{E}$ ,  $u(x, y)$  has first derivatives Hölder continuous to  $\mathcal{O}$ . Note that no growth condition is imposed in any of this work.

If  $2\alpha > \pi$  then it can occur that a central fan of opening  $\pi$  appears, in addition to the two fans at the sides.

### Pendent Drops

We consider what happens when  $\kappa < 0$  in (3). That occurs when the heavier fluid lies above the interface. Examples are a liquid drop hanging from a “medicine dropper”, or a drop pendent from a horizontal plate. The behavior of such solutions is very different from what occurs in the cases discussed above and, in general, instabilities must be expected. This “pendent drop equation” was much studied toward the end of the last century, and Kelvin calculated a remarkable particular solution of a parametric form of the equation; see Figure 14.

This surface is unstable; however its bottom tip could be observed as a stable drop hanging from a ceiling in a house with a leaking roof. The best stability criteria were obtained in 1980 by Wentz, who showed that in the development of a drop by increasing volume, *instability occurs after the initial appearance of an inflection in the profile, and prior to appearance of a second inflection.* Wentz showed existence of stable drops with both “neck”



**Figure 15. Stable pendent drop exhibiting inflection on the profile, also neck and bulge.**

and “bulge”. An example is the drop of colored water in a bath of castor oil, shown in Figure 15.

Concus and Finn proved the existence of “Kelvin drops” that are formal solutions of the parametric equation, and which have an arbitrarily large number of bulges. In addition they proved existence of a rotationally symmetric singular solution  $U(r) \approx 1/\kappa r$  of (4); this solution was shown by M.-F. Bidaut-Veron to extend to a strict solution for all  $r > 0$ . (If  $\kappa \geq 0$  then any isolated singularity of a solution of (3) is removable.) It was shown by Finn that in the limit as the number of bulges increases unboundedly, the Kelvin solutions tend, uniformly in compacta, to such a singular solution. In a remarkable work now in preparation, R. Nickolov proves the uniqueness of that singular solution, among all rotationally symmetric surfaces with a nonremovable isolated singularity. The result holds without growth hypotheses.

### Gradient Bounds

In addition to the height bounds indicated in Theorems 2, 3, and 4, gradient bounds can also be obtained. Again, some of these have an inimical character, reflecting the particular nonlinearity of the problems. We indicate two such results:

i) (Finn and Giusti, 1977). *There exists  $R_0 = (0.5654064\dots)/H_0$  and a decreasing function  $G(RH_0)$  with  $G(R_0H_0) = \infty$  and  $G(1) = 0$ , such that if  $u(x, y)$  satisfies (9) with  $H = H_0 \equiv \text{const.} > 0$  in a disk  $B_R(0)$  and  $R > R_0$ , then  $|Du(0)| < G(RH_0)$ . The condition  $R > R_0$  is necessary. There is no solution of (9) in  $B_R(0)$  if  $RH_0 > 1$ .*

ii) (Finn and Lu, 1998). *Suppose  $H = H(u)$  with  $H'(u) \geq 0$  and  $H(-\infty) \neq H(+\infty)$ . Then there exists  $\mathcal{F}(R) < \infty$  such that if  $u(x, y)$  satisfies (9) in  $B_R(0)$  then  $|Du(0)| < \mathcal{F}(R)$ .*

From the case  $R < R_0$  in (i) we see that the estimate of (ii) would be false if  $H$  is identically constant. We note that the hypotheses of (ii) are satisfied by the equation (4) for capillary surfaces in a gravity field when  $\kappa > 0$ .

### Past and Future

I have described only some of the many new results that have appeared in recent years; choices had to be made as to what to cover, and they were based largely on the simple criterion of familiarity. Other directions of interest can be inferred from items in the bibliography. Let me close with the opening quotation from the 1851 Russian treatise on capillarity by A. Yu Davidov:

The outstanding contributions made by Poisson and by Laplace to the mathematical theory of capillary phenomena have completely exhausted the subject and brought it to such a level of perfection that there is hardly anything more to be gained by its further investigation.

For the later French and German translations of the book, Davidov changed the quotation to:

The outstanding contributions made by Poisson, by Laplace, and by Gauss to the mathematical theory of capillary phenomena have brought the subject to a high level of perfection.

The subject has advanced in significant ways since the time of Davidov, but may nevertheless still be in early stages. The material I have described should indicate the kind of behavior to be expected; some of it may serve as building blocks toward creation of a cohesive and structured theory.

### Acknowledgments

The work described here was supported in part by grants from the NASA Microgravity Research Division and from the NSF Division of Mathematical Sciences. I am indebted to many colleagues and students for numerous conversations, extending over many years, that have deepened my knowledge and understanding. I wish to thank the editors of the *Notices* for careful reading of the manuscript and for perceptive comments from which the exposition has benefited greatly. The exposition has also profited from comments by Paul Concus and by Mark Weislogel.

—R. F.

### Skeletal Bibliography

- [1] E. GIUSTI, *Minimal Surfaces and Functions of Bounded Variation*, Birkhäuser-Verlag, Basel, Boston, 1984.
- [2] U. MASSARI and M. MIRANDA, *Minimal Surfaces of Codimension One*, North-Holland, Amsterdam, New York, 1984.

- [3] R. FINN, *Equilibrium Capillary Surfaces*, Springer-Verlag, New York, 1986; Russian translation (with appendix by H. C. Wente), Mir Publishers, 1988.
- [4] R. FINN and R. NEEL, Singular solutions of the capillary equation, *J. Reine Angew. Math.*, to appear.
- [5] R. FINN and J. MCCUAN, Vertex theorems for capillary surfaces on support planes, *Math. Nachr.*, to appear.
- [6] P. CONCUS, R. FINN, and J. MCCUAN, Liquid bridges, edge blobs, and Scherk-type capillary surfaces, Stanford University preprint, 1999.
- [7] K. LANCASTER and D. SIEGEL, Existence and behavior of the radial limits of a bounded capillary surface at a corner, *Pacific J. Math.* **176** (1996), 165–194; editorial corrections in *Pacific J. Math.* **179** (1997), 397–402.
- [8] T. STÜRZENHECKER, Existence of local minima for capillarity problems, *J. Geom. Anal.* **6** (1996), 135–150.
- [9] A.D. MYSHKIS, V.G. BABSKIĬ, N.D. KOPACHEVSKIĬ, L.A. SLOBOZHANIN, and A. D. TYUPTSOV, *Low-Gravity Fluid Mechanics. Mathematical Theory of Capillary Phenomena*, translated from the Russian by R. S. Wadhwa, Springer-Verlag, Berlin, New York, 1987.
- [10] F. ALMGREN, The geometric calculus of variations and modeling natural phenomena, *Statistical Thermodynamics and Differential Geometry of Microstructural Materials (Minneapolis, MN, 1991)*, IMA Vol. Math. Appl., vol. 51, Springer, New York, 1993, pp. 1–5.
- [11] K. GROSSE-BRAUCKMANN, *Complete Embedded Constant Mean Curvature Surfaces*, Habilitationsschrift, Universität Bonn, 1998.

### About the Cover

The top row exhibits “nearly discontinuous” dependence on data for fluid in a cylindrical “canonical proboscis” container in zero gravity; the container section has two noses with slightly different critical angles that encompass the one for the fluid. Following successive taps by the astronaut, the fluid remains bounded in height below a predicted maximum on one side, but rises well above that height on the other side.

The second row shows symmetry breaking for fluid in an “exotic container” designed for zero gravity, shown just prior to and near the end of free fall in a drop tower. The curves on the lower left are calculated meridional sections of a continuum of symmetric equilibrium surfaces bounding equal volumes in the container; all these surfaces are unstable. The fluid volume for the drop tower experiment is chosen so that the initial section in the earth’s gravity field can be identical to the horizontal section of the calculated zero gravity family.

The lower right shows comparison of calculation and experiment for surfaces yielding asymmetrical critical points for mechanical energy in an exotic container during an experiment on the Mir Space Station. The apparent global minimum (“spoon”) and a local minimum of larger energy (“potato chip”) are both observed by the astronaut.

The cover montage was prepared by Gary Nolan of the NASA Glenn Research Center.

—R. F.

